ELECTRONIC SUPPORTING INFORMATION

Size-dependent Luminescence in HfO_2 Nanocrystals: towards White Emission from Intrinsic Surface Defects

Irene Villa[†$], *Anna Vedda*[†], *Mauro Fasoli*[†], *Roberto Lorenzi*[†], *Niklaus Kränzlin*[‡], *Felix Rechberger*[‡], *Gabriele Ilari*[▼], *Darinka Primc*[‡], *Bodo Hattendorf*[‡], *Florian J. Heiligtag*[‡], *Markus Niederberger*[‡], *Alessandro Lauria*[‡*]

[†]Department of Materials Science, University of Milano-Bicocca, Via R. Cozzi 55, 20125 Milano, Italy.

[‡]Laboratory for Multifunctional Materials, Department of Materials, ETH Zürich, Vladimir-Prelog-Weg 5, 8093 Zürich, Switzerland.

[▼]Electron Microscopy Center, EMPA, Swiss Federal Laboratories for Materials Science and Technology, 8600 Dübendorf, Switzerland

[‡]Department of Chemistry and Applied Biosciences, Laboratory of Inorganic Chemistry, ETH Zurich, Vladimir-Prelog-Weg 1, 8093 Zurich, Switzerland

EXPERIMENTAL

Materials

Hafnium(IV) tert-butoxide (99.99%+Zr) was purchased from Multivalent Laboratory, Eriswell, UK. Anhydrous Benzyl alcohol (99.8%) was purchased from Sigma-Aldrich. Krypton (99.999%) and nitrogen (99.999%) were provided by PanGas AG, Switzerland.
All precursors were used as received without further purification.

Synthesis of HfO_2 nanoparticles

Syntheses by nonaqueous sol-gel were carried out in a glove box (O_2 and H_2O < 0.1 ppm). In a typical synthesis, hafnium(IV) t-butoxide was added to anhydrous benzyl alcohol (BnOH) into a glass test tube. For the 0.75 mol% Ti-doped sample, the appropriate amount of $TiCl_3$ (Sigma-Aldrich) was mixed to the solvent before addition of Hf precursor. A total amount of 2.4 mmol of precursors and a volume of 20 mL BnOH were used. The reaction mixture was transferred into a Teflon liner of 45 mL, slid into a steel autoclave (acid digestion vessel mod. 4744 by Parr Instrument Company, USA) and carefully sealed. The autoclave was taken out of the glove box and heated in a furnace at 220 °C for 96 hours. The synthesis resulted on a milky suspension that was centrifuged; the precipitate thoroughly washed with diethyl ether (Aldrich), then dried in air at 60 °C overnight.

Annealing

The powders were placed in quartz crucibles and heated in a muffle oven with a heating rate of 10 °C /min, the samples was kept at the final temperature for 2 hours. Temperatures from 400 up to 1000 °C were considered.

XRD analysis

The PXRD studies performed to investigate the temperature dependent phase evolution of the HfO_2 nanoparticles were conducted on a X'Pert Pro powder diffractometer (PANalytical B.V., The Netherlands) equipped with a high-temperature oven-chamber HTK 1200 (Anton Paar GmbH, Austria) containing the analyzed powder supported on an alumina sample holder. The diffractometer was operated in reflection mode under constant irradiated volume conditions with Cu Kα radiation (45 kV, 40 mA).

in situ analysis: The sample was heated from RT to 1000 °C meanwhile every 100 °C a PXRD scan was recorded. At each temperature the sample was given 10 min. for equilibration before the measurement started. The subsequent PXRD scan took 20 min.

ex situ analysis: After annealing the samples in a muffle oven to the corresponding temperatures, they were allowed to cool down under ambient conditions. Subsequently introduced into the high-temperature oven-chamber, all PXRD scans were recorded at room temperature.

XRD Data Handling

For evaluating the recorded diffractograms, multiple peak fitting routine was applied in order to extract full width at half maximum (FWHM) values. The peak analyzer function within the OriginPro software package (*OriginPro v. 8.6.0, OriginLab Corporation USA*) was used to fit a pseudo-voigt profile to the corresponding peaks. The crystallite sizes were calculated after

Scherrer using the FWHM values extracted from the hafnia (-111) peaks at 28 degrees. An estimate of the error was made by attributing given uncertainties to the corresponding variables inserted into the Scherrer equation (see Table S1).

Tab S1. Attributed uncertainties of the variables used for calculating the average crystallite size after Scherrer

Variable	Mean value	Uncertainty
Scherrer Constant K	0.85	0.15 given the fact that the actual crystal shape is unknown the range of values for K for the most representative shapes is considered [Langford J. I. and Wilson A. J. C. *J. Appl. Cryst.* 1978, 11, 102-113]
Wavelength X-ray source λ	1.5418E-10	-
FWHM	From fitting result	From fitting result
Position of peak maximum height Θ	From fitting result	From attributing an accuracy of 0.1 to the measured peak position due to possible misalignment of the sample and/or inaccurate movement of the sample stage.

BET Specific Surface Analysis

Prior to determining the surface area, the samples were outgassed at 120 °C for at least 12 h and krypton gas sorption measurements at 77 K were carried out on a Quantachrome Autosorb iQ. For selected samples with sufficient surface area, the measurements were confirmed by nitrogen gas sorption. The surface area was calculated via a multipoint Brunauer-Emmet-Teller (BET) method.

TEM analysis

For the HRTEM investigation the products (colloidally stabilized HfO_2 nanoparticles or fine-grained calcined particles redispersed in iso-propanol) were deposited on a copper-grid-supported perforated transparent carbon foil. A field emission electron-source transmission electron microscope (JEOL 2010F) was operated at 200 kV. The STEM images in Fig. S5 were recorded on a JEOL 2200 STEM/TEM field emission microscope operated at 200 kV.

Vibrational spectroscopy

Attenuated total reflectance (ATR) measurements were performed on a Bruker Alpha FT-IR Spectrometer equipped with diamond ATR optics. MicroRaman spectra were collected using an InVia Raman Microscope from Renishaw (UK) at room temperature in backscattering configuration, equipped with a 532 nm laser line.

LA-ICPMS analyses Ti in Hafnia

The mass fraction of Ti with respect to Hf (and Zr) was determined by Laser Ablation Inductively Coupled Plasma Mass Spectrometry (LA-ICPMS) using a Geolas C 193 nm laser ablation system (Coherent, Göttingen, D) connected to an Element XR (Thermo Fisher, Bremen, D) sector field ICPMS. Operating conditions are given in table 1. For each sample randomly chosen spots were targeted and material ablated in helium atmosphere for periods of at least 40 seconds. The ablated sample aerosol was transported to the ICPMS via 1 m flexible tubing after addition of the argon make-up gas. ^{49}Ti was evaluated for quantification to avoid a substantial interference from doubly charged Zr that were observed in the ICPMS spectra and overlap with the more abundant isotopes of Ti. Data acquisition was performed in time resolved mode by first recording the signal for the gas blank only for at least 30 seconds before starting the ablation[1]. Sensitivity ratios for Zr and Ti relative to Hf were determined by ablating SRM NIST 610 and using Georem [2] preferred concentration values of Ti, Zr and Hf. The SRM NIST 610 was measured twice at the beginning and the end of a sequence of 16 individual analyses to monitor instrument drift. While absolute sensitivities in LA-ICPMS may vary by 10s of % during an analytical session, the relative sensitivities of Ti and Zr to Hf remained practically constant with < 5% change of the course of these analyses. The wide-range detection system of the ICPMS was cross-calibrated before the analysis using the procedure recommended by the manufacturer. All signals obtained during ablation were background corrected using the respective gas blank acquired before the ablation. Sensitivity ratios obtained from the SRM NIST 610 were determined and used to calculate mass fractions of Ti and Zr relative to Hf according to:

$$\frac{m[Ti,Zr]_S}{m[Hf]_S} = \frac{I[Ti,Zr]_S \times c[Ti,Zr]_R \times I[Hf]_R}{I[Hf]_S \times c[Hf]_R \times I[Ti,Zr]_R}$$

m: mass, *I*: Net ion signal, *c*: concentration, *S*: Hafnia Sample, *R*: NIST SRM 610 reference

Table : operating conditions

Laser Ablation GeoLas C	
Wavelength	193 nm
Energy density	6 J/cm^2
Spot size	90 mm
Laser Repetition rate	10 Hz
Carrier gas flow rate	1.05 L/min He
ICPMS Element XR	
Rf-Power	1450 W
Coolant gas flow rate	16 L/min Ar
Auxiliary gas flow rate	0.9 L/min Ar
Make-up gas flow rate	1.2 L/min Ar

Mass resolution setting	low
Isotopes monitored	^{48}Ti, ^{49}Ti, ^{91}Zr, ^{178}Hf
Mass / integration window	50% / 40%
Samples / peak	80
Dwell time / sample	1 ms

[1] H. P. Longerich, S. E. Jackson and D. Günther, Laser Ablation Inductively Coupled Plasma Mass Spectrometric Transient Signal Data Acquisition and Analyte Concentration Calculation, J. Anal. At. Spectrom. 11 (9), 899-904 (1996).

[2] Georem Database, Geological and Environmental Reference Materials, http://georem.mpch-mainz.gwdg.de/

Optical Characterization

All samples were dried in air at 150 °C for 15 h prior to optical measurements in order to desorb humidity and moisture. Steady state PL spectra were measured at RT by a xenon lamp as excitation source, together with a double monochromator (Jobin-Yvon Gemini 180 with a 1200 grooves/mm grating), and recorded through a nitrogen cooled CCD detector coupled to a monochromator (Jobin-Yvon Micro HR). Time-resolved PL spectra (5 nm of bandwidth), and PL decay (20 nm of bandwidth at 490 nm) were collected by means of an Edinburgh FLS980 fluorescence spectrometer operating in Time Correlated Single Photon Counting configuration with pulsed LED source at 250 nm or 340 nm (pulse duration 600 ps, repetition rate 100 ns or 50 μs). The same instrument setup was adopted for the collection of emission spectra used for the evaluation of quantum yields. We used a LED at 340 nm as excitation source with an emission bandwidth of 20 nm. Quantum yields (QY) were measured by using the method described in Ref. S1. Incident light power R_{STD} has been evaluated by measuring the signal, integrated in the range 300-390 nm, of a reference sample of MgO acting as diffuser. Then PL of the samples were collected in the same experimental condition and geometry. The QY was finally calculated with the following formula:

$$QY = \frac{E}{(R_{STD} - R_{SMPL})}$$

where R_{SMPL} and E are the integrated signals over the source (300-390 nm) and emission (390-700 nm) spectral range, respectively. Quantum efficiency (QE) was instead calculated as the ratio between emitted and incident photons ($QE = E/R_{STD}$). All spectra were corrected for monochromator and detector response. The relative error on QY measurement has been estimated to be 25% assuming the same consideration of Ref. S1, such as reflectivity of diffuser not exactly equal to unity, partial reflection of the window quartz placed in front of the powdered sample holder, and particle size effects. Measure accuracy of the system has

been verified by measuring the QY of sodium salicylate (Sigma Aldrich) excited at 250 nm and obtaining a value of 68 ± 17%, in accordance with data reported in literature (Ref. S2 and S3) of 55 - 64%.

Decay time in the msec domain were collected by means of a Cary Eclipse spectrofluorometer with a Xenon microsecond flash lamp as light source, monitoring the signal with a photomultiplier tube operating at 600 V, and 5 nm of bandwidth both in excitation and emission. Phosphorescence emission and excitation spectra were collected in the same condition with total decay time, time delay, and gate time of 30 ms, 0.25 ms, and 5 ms, respectively. Time decays in the msec domain were fitted, after normalization, with a triple-exponential decay:

$$f(t) = ae^{-t/\tau_1} + be^{-t/\tau_2} + ce^{-t/\tau_3} \qquad \text{Eq. S1}$$

Fitting results for HfO_2 treated at 450 °C with excitation at 250 nm and monitored at maxima registered in phosphorescence (430 nm and 530 nm) and fluorescence (490 nm) spectra are summarized in the following table:

Table S2. Fitting results of decay profile in the ms domain according to Eq.S1 for HfO_2 sample treated at 450 °C.

	a	*b*	*c*	τ_1 (ms)	τ_2 (ms)	τ_3 (ms)
Exc 250 nm (4.96 eV) Emi 430 nm (2.86 eV)	0.163	0.404	0.407	10.8	1.97	0.271
Exc 250 nm (4.96 eV) Emi 490 nm (2.5 eV)	0.234	0.387	0.360	11.3	2.10	0.238
Exc 250 nm (4.96 eV) Emi 530 nm (2.34 eV)	0.284	0.406	0.306	11.5	2.04	0.198

References:

Ref. S1 - “Technique for the determination of absolute emission quantum yields of powdered samples”, Mark S. Wrighton , David S. Ginley , David L. Morse, J. Phys. Chem., 1974, 78 (22), pp 2229–2233

Ref. S2 – “Determination of the absolute quantum efficiency of luminescence of solid materials employing photoacoustic spectroscopy”, M. J. Adams, J. G. Highfield, G. F. Kirkbright, Anal. Chem., 1980, 52 (8), pp 1260–1264

Ref S3 - "Absolute Quantum Yield of Sodium Salicylate," N. Kristianpoller, J. Opt. Soc. Am. 54, 1285-1286 (1964)

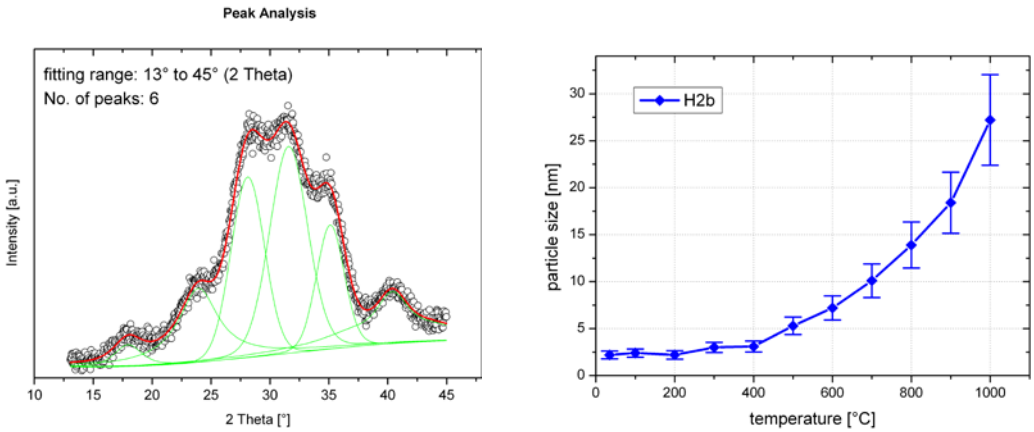

Figure S1. Left panel: example of diffractograms analysis for the determination of average grain size through the Scherrer formula (here the fit for determining the single reflection [-111] at 28° is shown for the measurement taken at 100 °C). Right panel: average crystal sizes depending on T, obtained by the Scherrer formula on in situ XRD after fitting.

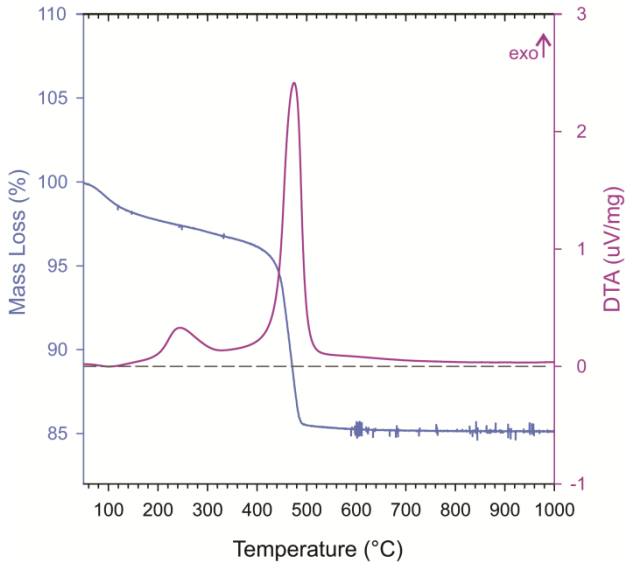

Figure S2. TGA/DTA curves recorded on undoped HfO_2 nanoparticles recorded using a heating rate of 10 °C/min. The two main exothermic events occurring in the range 200-520 °C represent the evaporation and oxidative decomposition of benzoate residuals, to which corresponds a total weight loss of 15%.

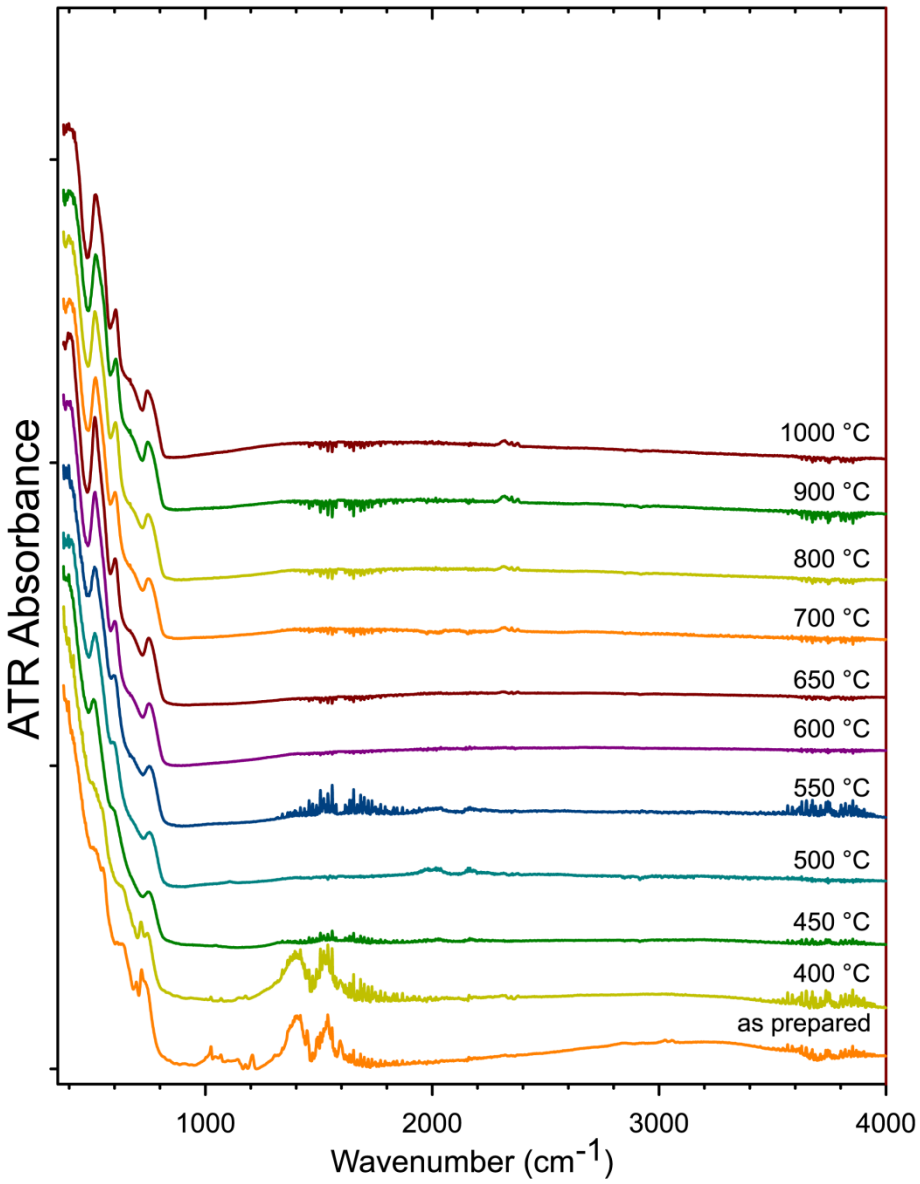

Figure S3. ATR-FTIR of HfO_2 powders treated at different temperatures. The benzoate surface coverage of the particles is visible in the "as prepared" sample spectrum through vibrational modes in the range 1000-1700 cm^{-1} , not observed for samples treated at 500 °C and above. (Artifacts in the range 1250-1800; 3600-3900 cm^{-1} and at 2250 cm^{-1} arise from air humidity and carbon dioxide, respectively).

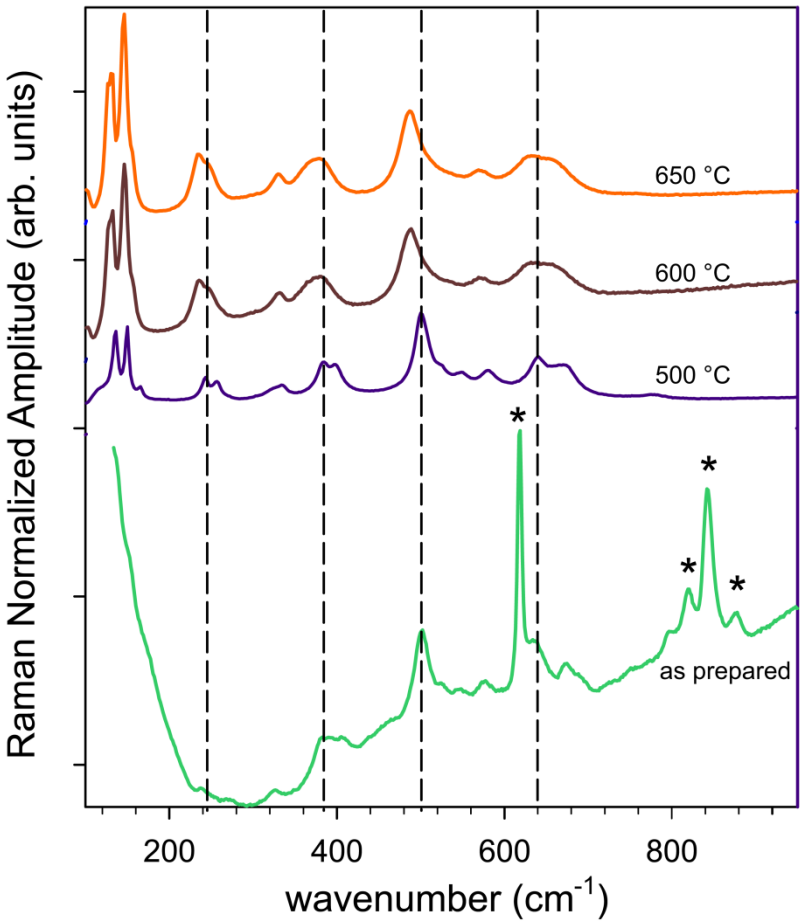

Figure S4. Raman spectra recorded on HfO_2 NPs treated at different temperatures, namely from bottom to top: as prepared NPs (green curve) with benzoate capping, NPs treated at 500 °C (blue curve), at 600 °C (brown curve), and 650 °C (orange curve). The benzoate peaks visible in the untreated sample (marked with stars) disappear after annealing. Dashed lines indicate the typical spectral positions of hafnia vibrational modes for the lowest and the highest annealing temperatures. The annealing at temperatures of 600 and 650 °C, reveal Raman modes slightly broadened and shifted towards lower wavenumbers, possibly indicating a lower level of mid-range order of the nanocrystalline lattice, and altered interatomic distances.

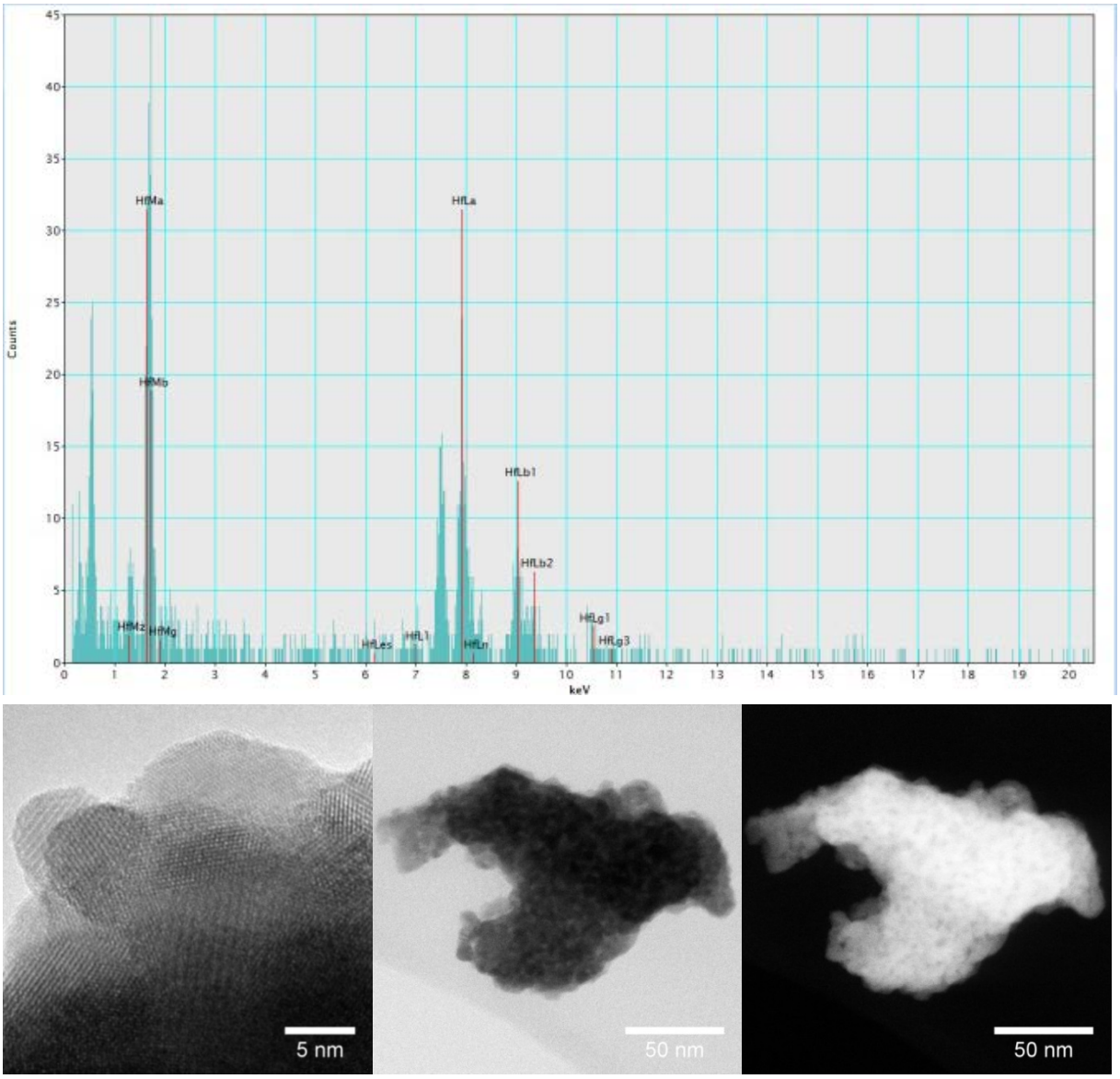

Figure S5. *ex situ* TEM analysis of HfO_2 nanopowders calcined at 550 °C. Top left: EDX spectrum of agglomerated nanocrystals revealing the composition rich in Hf (the peak at 7.47 KeV derives from Ni grids). Bottom left: HR-TEM micrograph showing very high crystallinity of the particles with a size of around 5-10 nm, in good agreement with the values obtained by Scherrer analysis of the XRD patterns for the same sample. Bottom center and bottom right: bright field STEM and HAADF micrographs, respectively, of the same sample showing the high residual porosity of the material responsible for high specific surface area, confirming that at this temperature the thermal treatment induces only partial surface reconfiguration/sintering.

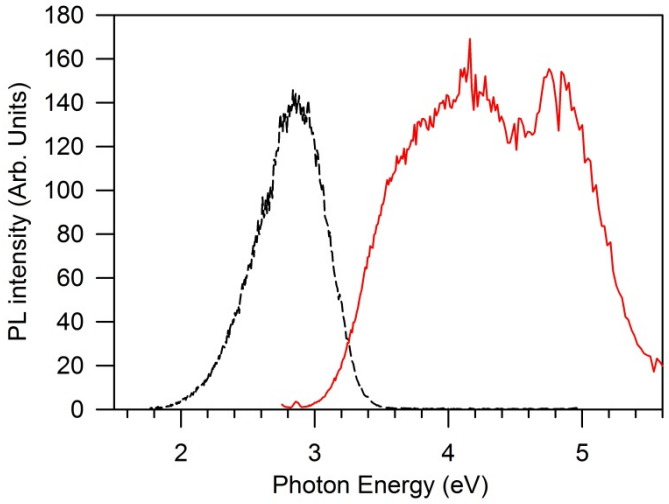

Figure S6. Phosphorescence excitation (red solid line, λ_{em} = 433 nm) and emission (black dashed line, λ_{exc} = 250 nm) spectra of HfO_2 nanopowder treated at 450 °C. Measurements recorded after 0.25 ms.

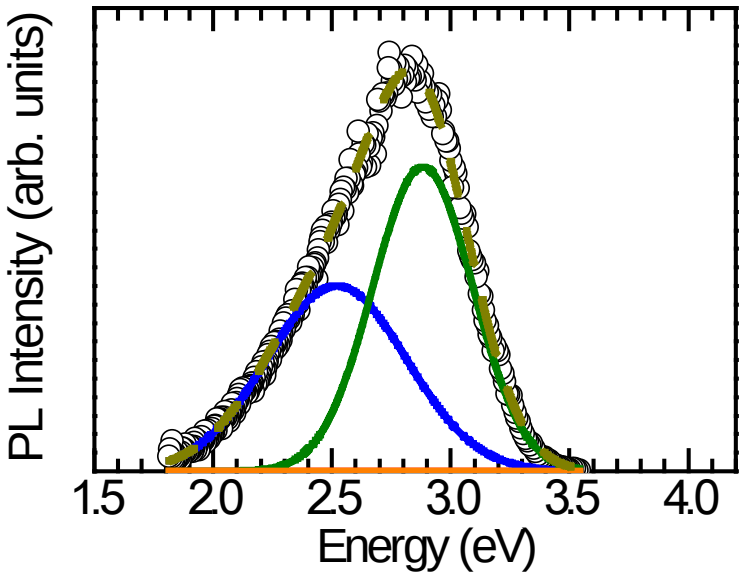

Figure S7. Deconvolution of phosphorescence emission spectrum of HfO_2 nanopowder treated at 450 °C excited at 250 nm, fitting results are reported on the last line of Table S3. The spectrum can be deconvolved into two Gaussian components, one at 2.5 eV, as reported in the Fig 2 and the second one at 2.88 eV which dominates the spectrum and is likely attributable to the same emission channel at 2.9 eV observed in steady-state measurements.

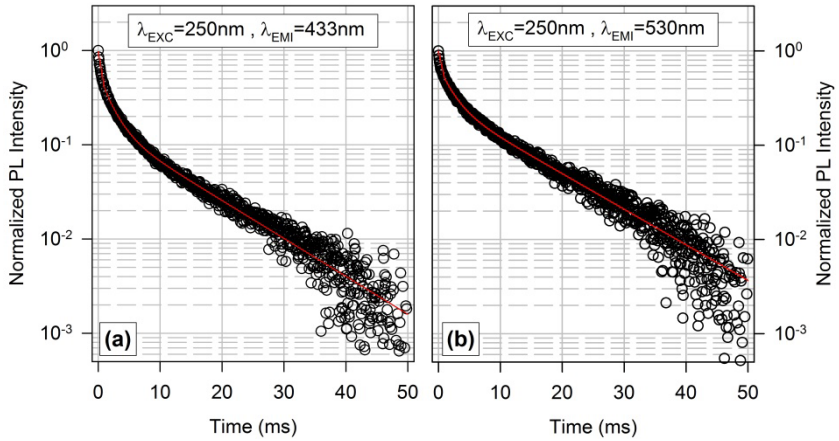

Figure S8. Time-resolved PL spectra of HfO_2 sample treated at 450 °C excited at 250 nm and monitored at 433 nm (a) and 530 nm (b). Red lines represent fitting result with fitting parameters reported in Tab. S2 and calculated according to Eq. S1.

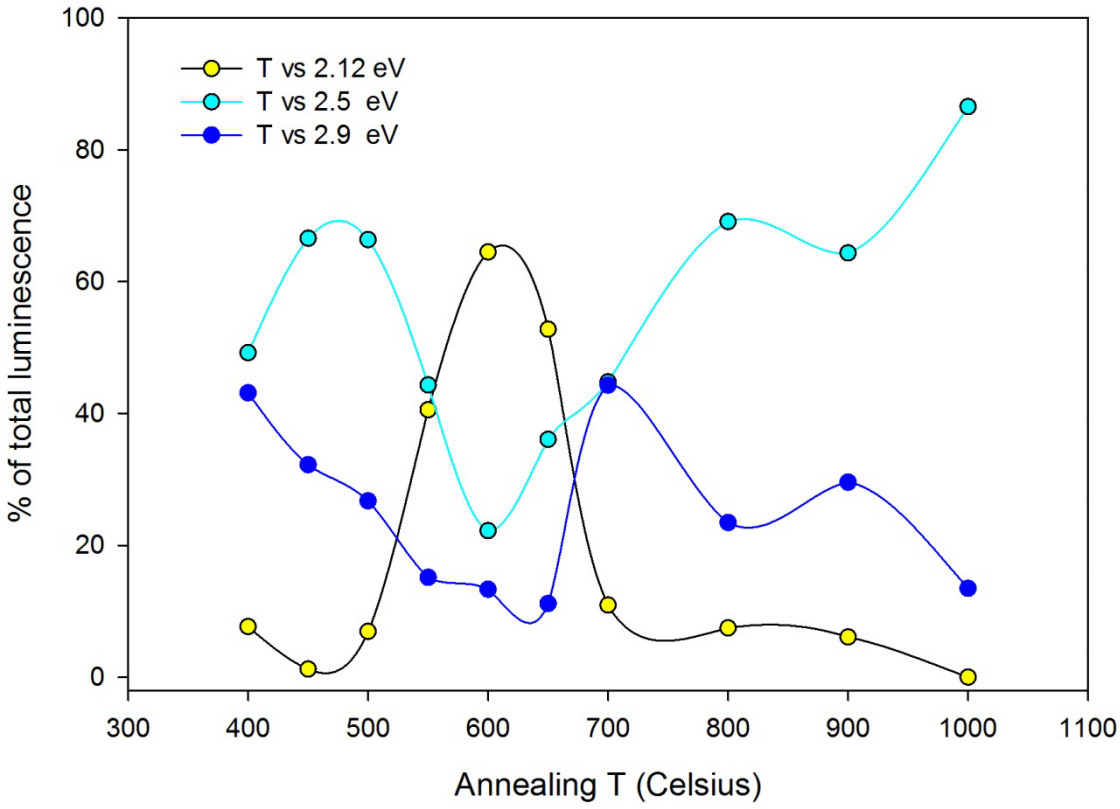

Figure S9. Spectral composition of the luminescence stimulated by 350 nm (3.54 eV) UV excitation depending on the annealing temperature. The emission integrals of each component are expressed as % of the total luminescence obtained as the sum of the three of them. More than 50% of the visible emission of samples treated between 550 and 650 °C is explained by the 2.12 eV (590 nm) component.

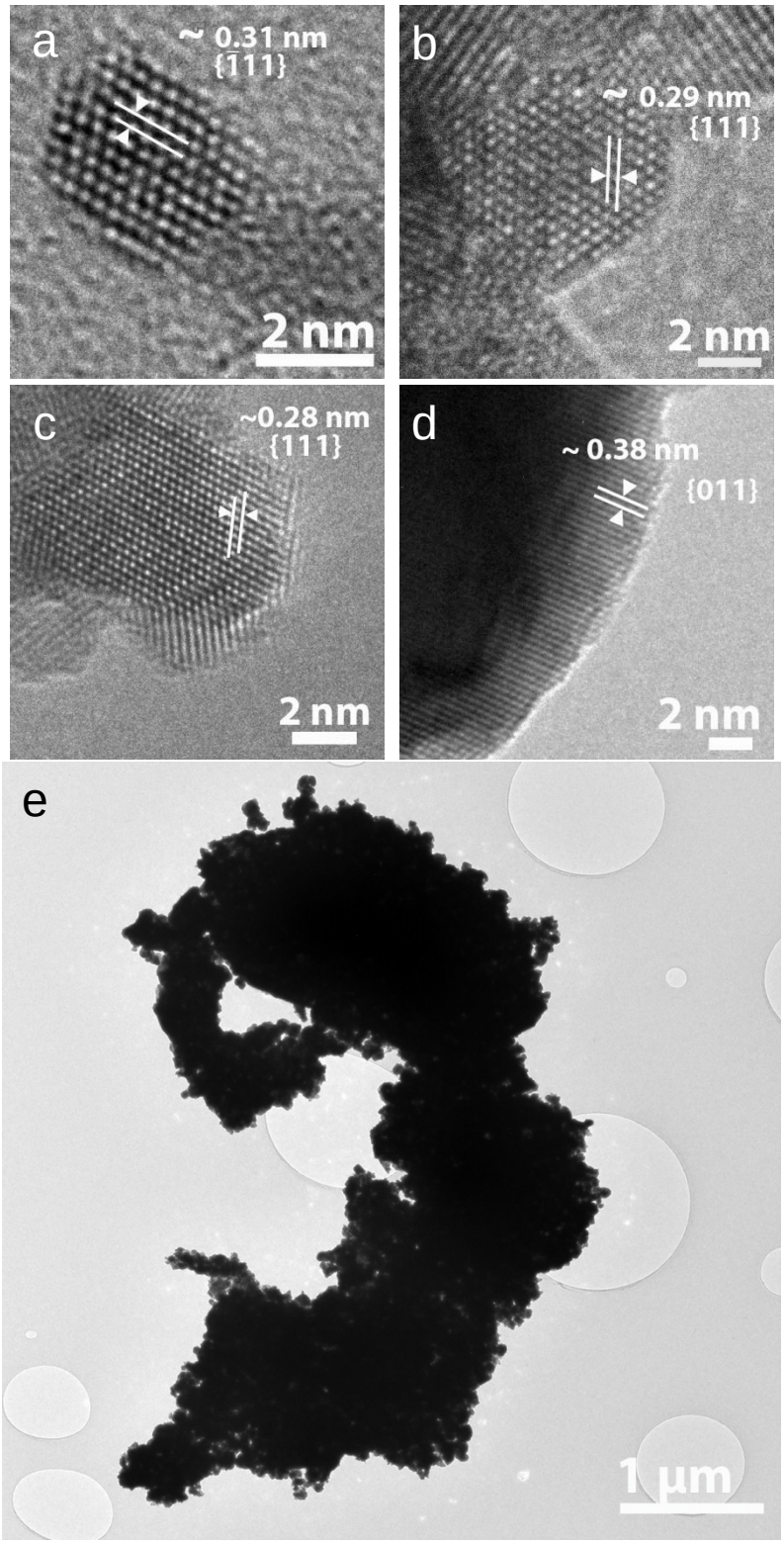

Figure S10: High resolution TEM images showing the crystallinity in hafnia samples. HR-TEM image "as prepared" hafnia nanoparticle (a) and powders heated at 400 °C (b), 500 °C (c), and 1000 °C (d). The periodicity of HR-TEM patterns for (a), (b-c) and (d) correspond to {-111}, {111} and {011} planes of monoclinic HfO_2 (JCPDS: 01-078-0050), respectively. A low magnification image on nanoparticles treated at 1000 °C (e) shows an overview of agglomerated nanocrystals (average crystal diameter 35nm).

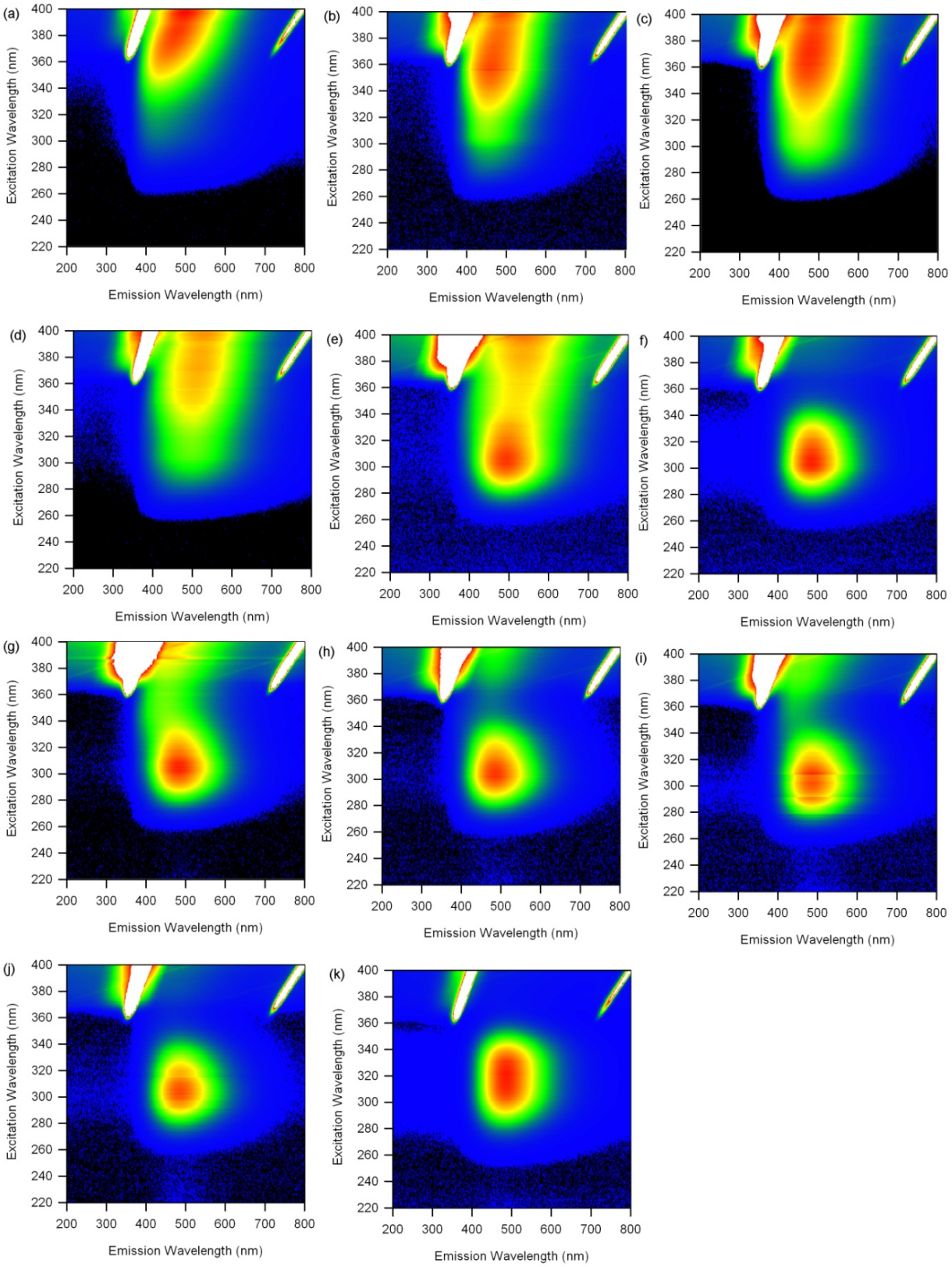

Figure S11: PL/PLE 3D plots of HfO_2 powders annealed at 400 °C (a), 450 °C (b), 500 °C (c), 550 °C (d), 600 °C (e), 650 °C (f), 700 °C (g), 800 °C (h), and 1000 °C (i). (j) PL/PLE 3D plots of HfO_2 powders doped with 0.75 mol% nominal Ti and annealed at 1000 °C.

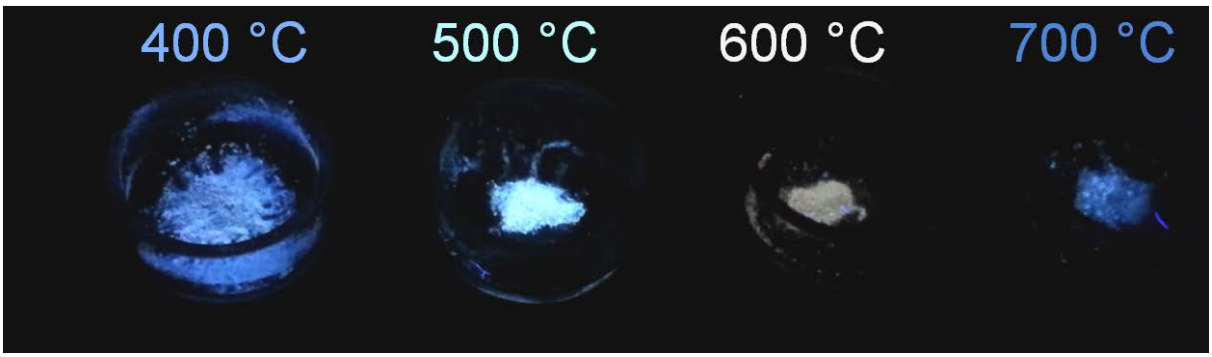

Figure S12. Optical image of HfO_2 nanopowders treated at different temperatures, under 365 nm UV illumination. The emission shifts from blue to white increasing the T up to 600 °C. Further increase of the temperature shifts the emission to blue again, accompanied by lower intensity.

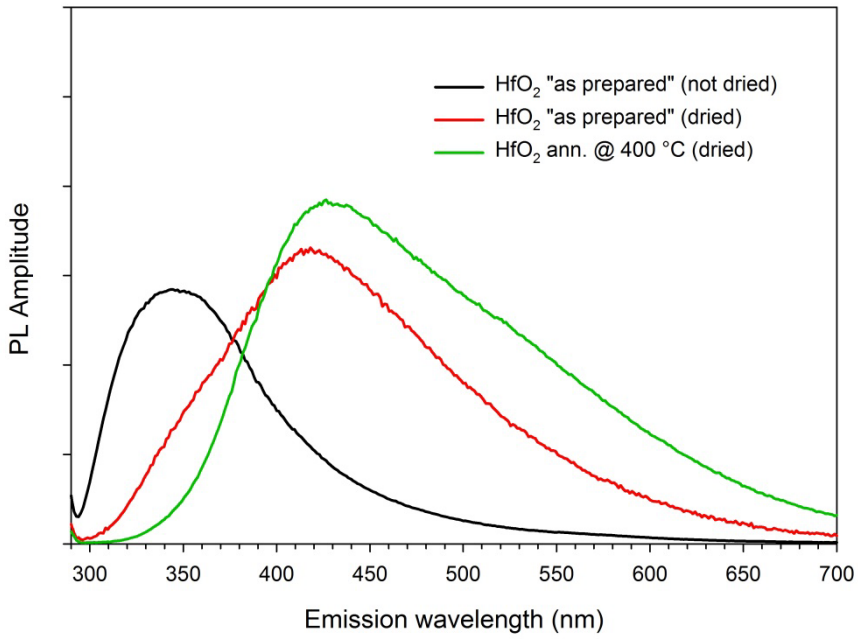

Figure S13. PL spectra of HfO_2 nanpowders. As prepared powders before any thermal treatment (black line), and after drying at 150 °C for 15h (red line). The PL of the powder annealed at 400 °C, and further dried, is shown for comparison (green line).

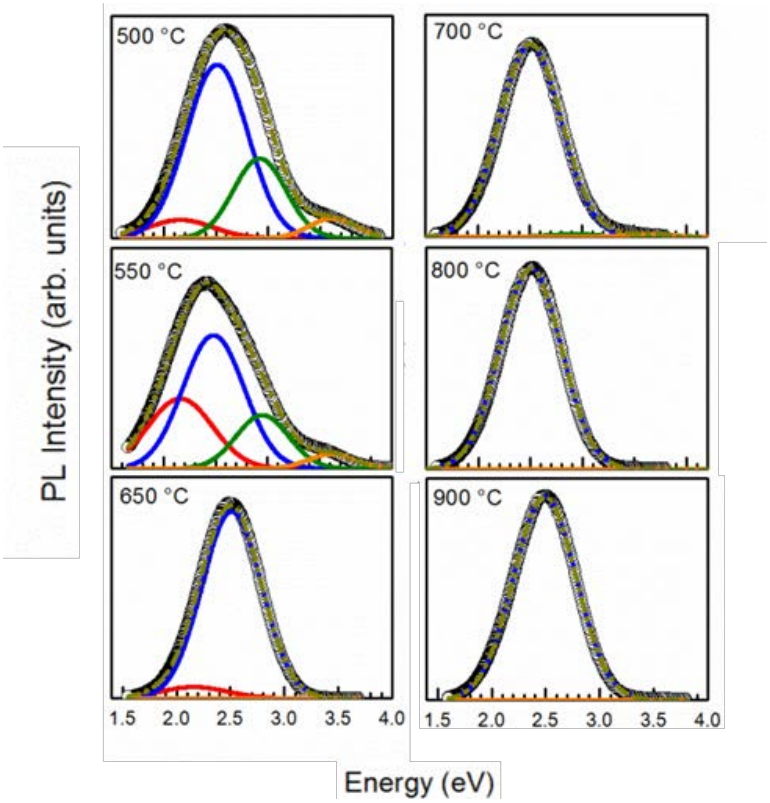

Figure S14. PL spectra of HfO_2 nanopowders treated at different temperatures, exciting at 280 nm (4.4 eV).

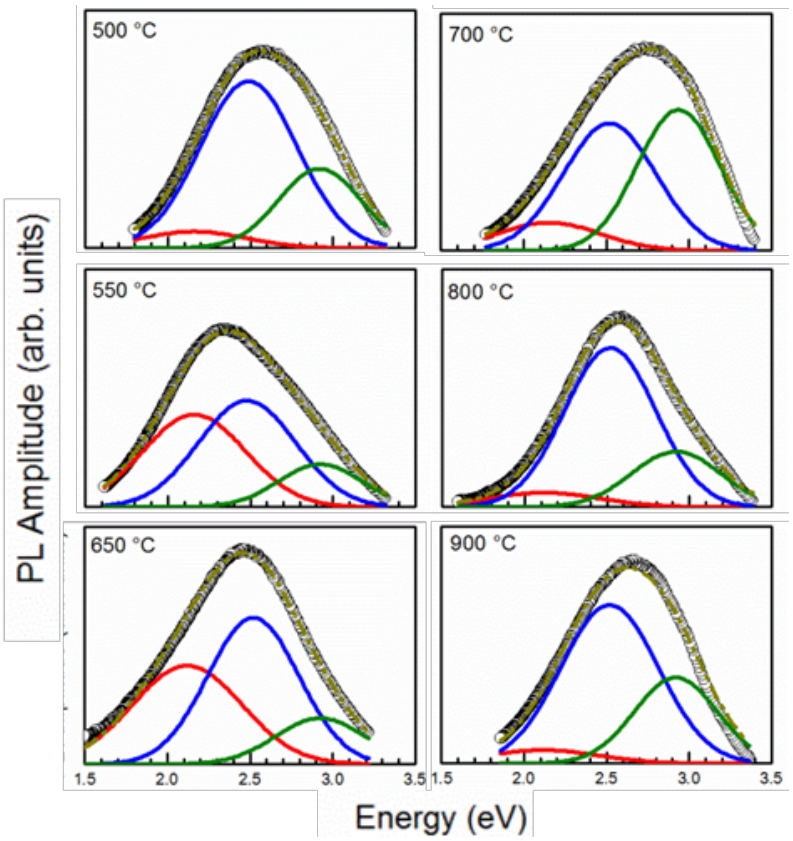

Figure S15. PL spectra of HfO_2 nanopowders treated at different temperatures, exciting at 350 nm (3.5 eV).

Table S3. Results of the Gaussian fit of the luminescence excited at 280 nm (4.4 eV). The last line refers to phosphorescence spectrum collected on sample treated at 450 °C and excited at 250 nm.

Samples	Band A		Band B		Band C		Band D	
	E (eV)	FWHM (eV)	E (eV)	FWHM (eV)	E (eV)	FWHM (eV)	E (eV)	FWHM (eV)
HfO_2:Ti @1000°C	---------	---------	2.51	0.66	---------	---------	---------	--------
1000°C			2.51	0.67				
900 °C	---------	---------	2.49	0.68	---------	---------	---------	---------
800 °C	---------	---------	2.50	0.69	---------	---------	---------	---------
700 °C	---------	---------	2.50	0.69	2.92	0.59	3.62	0.58
650 °C	2.16	0.73	2.51	0.65	---------	---------	---------	---------
600 °C	2.16	0.74	2.51	0.66	2.92	0.64	3.62	0.53
550 °C	2.16	0.73	2.48	0.69	2.95	0.60	3.62	0.53
500 °C	2.16	0.73	2.51	0.69	2.92	0.59	3.62	0.53
450 °C	2.12	0.78	2.52	0.59	2.92	0.59	3.66	0.53
400 °C	2.16	0.73	2.48	0.65	2.96	0.64	3.62	0.58
450 °C (Phos.)	---------	---------	2.52	0.59	2.88	0.42	---------	---------

Table S4. Results of the Gaussian fit of the luminescence excited at 350 nm (3.5 eV).

Samples	Band A		Band B		Band C	
	E (eV)	FWHM (eV)	E (eV)	FWHM (eV)	E (eV)	FWHM (eV)
HfO_2:Ti @1000°C	---------	---------	2.48	0.75	---------	---------
1000°C	2.12	0.78	2.51	0.69	2.92	0.59
900 °C	2.12	0.78	2.52	0.69	2.92	0.59
800 °C	2.12	0.78	2.52	0.65	2.92	0.64
700 °C	2.16	0.73	2.52	0.66	2.94	0.59
650 °C	2.16	0.78	2.51	0.65	2.93	0.64
600 °C	2.14	0.74	2.52	0.69	2.92	0.59
550 °C	2.16	0.73	2.48	0.68	2.92	0.59
500 °C	2.16	0.73	2.49	0.69	2.92	0.59
450 °C	2.12	0.78	2.52	0.69	2.92	0.59
400 °C	2.12	0.73	2.52	0.69	2.92	0.59

Table S5. CIE chromaticity coordinates (x,y) for the emission excited at 350 nm of HfO_2 nanopowders depending on the calcination final temperature. The values were obtained by correcting emission spectra with the CIE 1964 color matching functions.

Temperature (°C)	x	y
400	0.2067	0.2199
450	0.2026	0.2367
500	0.2231	0.2703
550	0.2838	0.3394
600	0.3146	0.3549
650	0.2635	0.3218
700	0.2092	0.2253
800	0.2134	0.2686
900	0.2113	0.2431
1000	0.2176	0.2820

Table S6. Fitting results of decay profile for HfO_2 samples (figure 4 in manuscript) treated at 450 °C and 900 °C and for HfO_2:Ti sample treated at 1000 °C. Time decays were fitted with a double-exponential decay: $f(t) = a \exp(-t/\tau 1) + b \exp(-t/\tau 2)$.

	a	b	t1	t2
HfO_2 @ 450 °C				
Exc 250 nm	0.92 ± 0.14	0.18 ± 0.03	1.7 ± 0.2 ns	7.4 ± 1.2 ns
Exc 340 nm	0.89 ± 0.13	0.18 ± 0.03	1.4 ± 0.1 ns	5.3 ± 0.5 ns
HfO_2 @ 900 °C				
Exc 250 nm	0.48 ± 0.07	0.43 ± 0.06	1.3 ± 0.2 µs	6.7 ± 0.2 µs
Exc 340 nm	1.05 ± 0.16	0.05 ± 0.01	1.3 ± 0.1 ns	7.7 ± 0.8 ns
HfO_2:Ti @ 1000°C				
Exc 250 nm	0.40 ± 0.06	0.48 ± 0.07	1.4 ± 0.2 µs	7.0 ± 0.8 µs